

On estimating the Shannon entropy and (un)certainty relations for design-structured POVMs

Alexey E. Rastegin*

Department of Theoretical Physics, Irkutsk State University, Irkutsk 664003, Russia

Complementarity relations between various characteristics of a probability distributions are at the core of information theory. In particular, lower and upper bounds for the entropic function are of great importance. In applied questions, we often deal with situations, where the sums of certain powers of probabilities are known. The main question is to how convert the imposed restrictions into two-sided estimates on the Shannon entropy. It is addressed in two different ways. More intuitive of them is based on truncated expansions of the Taylor type. Another method is based on the use of coefficients of the shifted Chebyshev polynomials. We conjecture here a family of polynomials for estimating the Shannon entropy from below. As a result, estimates are more uniform in the sense that errors do not become too large in particular points. The presented method is used for deriving uncertainty and certainty relations for POVMs assigned to a quantum design. Quantum designs are currently the subject of active researches due to potential applications in quantum information science. Other ways to use the proposed estimates are briefly discussed.

Keywords: complementarity relation, quantum design, Shannon entropy, Chebyshev polynomial

I. INTRODUCTION

The concept of entropy plays the fundamental role in statistical physics and information theory [1]. Irrespectively to the context of their use, entropic functions are hardly exposed to measure immediately. The latter is rather typical when one inspects deeper features, which are manifested only indirectly. Hence, we are interested in ways to connect entropic quantities with those characteristics that are easier to observe in practice. Results of such a kind constitute an essential part of information sciences, including quantum area [2]. Inequalities between entropy and index of coincidence is one of examples naturally raised in several ways [3]. Connecting inequalities between several information measures can also be used to choose properly a single notion appropriate in a particular context. The authors of [4] reviewed this issue with respect to quantum cryptography. Results of sufficiently general scope can often be improved in some special cases. In the following, we focus on the question of characterizing uncertainty and certainty relations for POVMs assigned to a quantum design.

Information entropies give a flexible tool to characterize genuine uncertainties in various situations [5]. Formulations of the Heisenberg uncertainty principle in entropic terms have attracted a considerable attention. For discrete observables, the entropic approach to uncertainty relations was reasoned in [6] and later developed in [7]. Basic results found in this area are reviewed in [8, 9]. For entropic uncertainty relations with continuous variables, see [10, 11] and references therein. In quantum information science, special types measurements have found a lot of attention. Mutually unbiased bases [12] and symmetric informationally complete measurements [13] are especially important examples. Quantum designs also called complex projective designs have been considered for several reasons [14, 15]. Characterizing uncertainties in design-structured POVMs is one of questions raised in this connection. The authors of [16] formulated uncertainty relations for such POVMs in terms of the Rényi and Tsallis entropies. Rényi formulation was improved in [17]. The results of [16, 17] also give entropic steering inequalities.

As the Rényi entropy cannot increase with growth of its order, uncertainty relations derived in [16, 17] imply estimates on the corresponding Shannon entropy from below. However, such estimates are sufficiently far from the optimal ones. The question of deriving uncertainty relations in terms of the Shannon entropy is beyond the methods of [16, 17]. The aim of this work is to address this question in detail. Moreover, the developed approach naturally lead to estimates on the corresponding Shannon entropy from above. In this sense, certainty relations for design-structured POVMs are formulated. The paper is organized as follows. In Section II, the two methods to get two-sided estimates on the Shannon entropy are considered. In particular, we conjecture polynomials whose coefficients are not determined according to Taylor's scheme. Section III is devoted to formulating uncertainty and certainty relations for POVMs assigned to a quantum design. These relations are released and compared with previous results within several examples. Applications to estimating the von Neumann entropy and steering inequalities are briefly mentioned.

*Electronic address: alexrastegin@mail.ru

Section IV concludes the paper. Some auxiliary material is presented in two appendices.

II. ON TWO-SIDED ESTIMATING THE SHANNON ENTROPY

In this section, we present two-sided estimates on the Shannon entropy in terms of the power sums of probabilities. Let us recall some basic definitions. The Shannon entropy of probability distribution $\mathbf{p} = \{p_j\}$ is defined as [18]

$$H_1(\mathbf{p}) := - \sum_j p_j \ln p_j. \quad (2.1)$$

For a pair of discrete random variables, the conditional entropy of X given Z reads as [18]

$$H_1(X|Z) := \sum_z p(z) H_1(\mathbf{p}_{X|z}), \quad (2.2)$$

where $\mathbf{p}_{X|z}$ consists of conditional probabilities $p(x|z)$. The authors of [3] introduced information diagrams that allow them to study relations between (2.1) and the index of coincidence

$$I^{(2)}(\mathbf{p}) := \sum_j p_j^2. \quad (2.3)$$

It is natural to consider a generalization of (2.3), namely

$$I^{(s)}(\mathbf{p}) := \sum_j p_j^s. \quad (2.4)$$

Such indices were briefly discussed in [3]. In the following, we will use (2.4) with integer $s \geq 2$. The quantity is directly connected with the Tsallis s -entropy defined as [19]

$$H_s(\mathbf{p}) := \frac{1}{1-s} \left(\sum_j p_j^s - 1 \right) = \frac{I^{(s)}(\mathbf{p}) - 1}{1-s}. \quad (2.5)$$

In the limit $s \rightarrow 1$, the latter reduces to (2.1). For a discussion of basic properties of (2.5) and other entropic functions, see section 2.7 of [20].

Suppose that several quantities of the form (2.4) are known exactly. It is natural to expect that these restrictions bound somehow available values of the Shannon entropy. Here, the main question is how to characterize possible entropic values explicitly. So, we try to express two-sided estimates on the entropic function in terms of indices of the form (2.4). In this work, we will base on the following idea. Suppose that we managed to find a polynomial $q(x)$ of degree n such that $q(0) = 0$ and

$$x \ln x \leq q(x) = \sum_{s=1}^n q_n^{(s)} x^s \quad (2.6)$$

for all $x \in [0, 1]$. It follows from (2.6) that

$$-q_n^{(1)} - \sum_{s=2}^n q_n^{(s)} I^{(s)}(\mathbf{p}) \leq H_1(\mathbf{p}). \quad (2.7)$$

It is useful to note that the inequality (2.6) simultaneously leads to estimating the Shannon entropy from above. Namely, we integrate both the sides of the inequality

$$1 + \ln \tilde{x} \leq 1 + \sum_{s=1}^n q_n^{(s)} \tilde{x}^{s-1} \quad (2.8)$$

from $\tilde{x} = x$ to $\tilde{x} = 1$, whence

$$-x \ln x \leq 1 + \sum_{s=1}^n \frac{q_n^{(s)}}{s} - x - \sum_{s=1}^n \frac{q_n^{(s)} x^s}{s}. \quad (2.9)$$

Similarly to (2.7), we then obtain

$$H_1(\mathbf{p}) \leq \sum_{s=2}^n \frac{q_n^{(s)}}{s} [1 - I^{(s)}(\mathbf{p})]. \quad (2.10)$$

When some indices of the form (2.4) are given, the maximal probability is inevitably bounded from above. Then both the relations (2.6) and (2.9) can be applied with rescaled probabilities. At this stage, however, we do not delve into this issue.

The main question is to find desired polynomials. At first glance, spline functions may seem an appropriate tool in this situation. However, their performance is good due proper selecting coefficients in many different ranges on which the interval of interest is divided. This is hardly applicable to the case, when probabilities *per se* are restricted only by fixing sums of some powers of them. To reach valid estimations, we have to take the maximum or the minimum of spline coefficients corresponding to the given power. Using suitable truncation of Taylor series is a natural way with rich history. Deficiencies of this approach come from the fact that truncated series gave very accurate results near the point of expansion but insufficient ones in peripheral regions [21]. Nevertheless, truncated expansions of the Taylor type are still a powerful tool for studying inequalities of interest. Instead, there are power expansions whose coefficients are not determined according to the Taylor scheme. In numerical analysis, such expansions are often based on the use of a suitable family of orthogonal polynomials. The significance of Chebyshev polynomials in various problems of applied analysis was clearly demonstrated by Lanczos [21]. Before addressing this idea, we complete the discussion of truncated expansions of the Taylor type.

Putting $1 - x = z \in [0, 1]$ and using the well-known expansion, we have

$$\ln x = \ln(1 - z) = - \sum_{r=1}^{\infty} \frac{z^r}{r} \leq - \sum_{r=1}^{n-1} \frac{z^r}{r}. \quad (2.11)$$

Multiplying the latter by $-x \leq 0$, one gets

$$f_n(x) \leq -x \ln x, \quad (2.12)$$

where

$$f_n(x) = x \sum_{r=1}^{n-1} \frac{(1-x)^r}{r} = \sum_{s=1}^n a_n^{(s)} x^s. \quad (2.13)$$

It is immediate to check that

$$a_n^{(1)} = \sum_{r=1}^{n-1} \frac{1}{r}, \quad a_n^{(s)} = (-1)^{s-1} \sum_{r=s-1}^{n-1} \frac{1}{r} \binom{r}{s-1} \quad (2 \leq s \leq n). \quad (2.14)$$

To estimate $(-x \ln x)$ from above, we could combine $-f_n(x) \leq x \ln x$ with (2.6) and (2.9). More direct way is to truncate the expansion of $(z-1) \ln(1-z)$. In any case, the result reads as

$$-x \ln x \leq h_n(x), \quad (2.15)$$

where

$$h_n(x) = (1-x) \left(1 - \sum_{r=1}^{n-1} \frac{(1-x)^r}{r(r+1)} \right) = \frac{1}{n} + \sum_{s=1}^n b_n^{(s)} x^s. \quad (2.16)$$

The coefficients are expressed as

$$b_n^{(1)} = \sum_{r=2}^{n-1} \frac{1}{r}, \quad b_n^{(s)} = \frac{(-1)^{s-1}}{s} \sum_{r=s-1}^{n-1} \frac{1}{r} \binom{r}{s-1} \quad (2 \leq s \leq n). \quad (2.17)$$

As obtained due to the Taylor scheme, the estimates (2.12) and (2.15) demonstrate a typical behavior. They give a very good approximation from own side in some left neighborhood of the point $x = 1$. In contrast, inaccuracies become comparatively large in a right neighborhood of the point $x = 0$. This is most obvious for (2.15) due to $h_n(0) = 1/n$. Thus, there is a certain asymmetry with respect to estimating in left and right regions of the range $x \in [0, 1]$. This asymmetry can be reduced due to the methods described in [21]. Although the inequalities (2.12) and (2.15) hold for $n = 1$, this value is not used in the following.

Let us proceed to the question of approximating with the use of orthogonal polynomials. This tool is known very well in the sense of expansions with rigid coefficients. That is, adding a next member of the used orthogonal family into our expansion does not affect the sum we have obtained before. In effect, the requirement of rigidity of coefficients

directly leads to the orthogonality condition. As a flip side of this circumstance, we have to deal with oscillating approximations. Here, one can only minimize an integral error, say, in the sense of least squares. Estimating the function of interest from one side or the other is beyond expansions with rigid coefficients. As was emphasized by Lanczos (see, e.g., chapter VII of [21]), the requirement of rigidity of coefficients received an exceptional attention rather for historical reasons. To reach more effective approximations, adding a next member should be combined with changing all the coefficients. So, we have arrived at expansions with flexible coefficients.

In §VII.12 of his book [21] Lanczos described the so-called τ -method to solve ordinary differential equations. The next paragraph of [21] is devoted to a variant of the τ -method with canonical polynomials. The matter of question is posed as follows. Let some function $x \mapsto y(x)$ obey certain ordinary differential equation. Then a suitable power expansion for this function can be obtained as an approximate solution of the given differential equation. When the original differential equation is not solvable in polynomials, it is modified by adding an inhomogeneous term. Lanczos showed how to deal with such a term chosen as one of the shifted Chebyshev polynomials. This procedure generally includes a certain freedom. We only note that the example considered leads to a useful power expansion of $y(x) = x \ln x$. Taking the equation

$$xy'(x) - y(x) = x \quad (2.18)$$

with the boundary condition $y(1) = 0$, one adds into the right-hand side the term $T_n^*(x)$. By $T_n^*(x)$, we mean here n -th shifted Chebyshev polynomial. Some facts about Chebyshev polynomials are listed in Appendix A. The procedure results in the sum

$$\frac{(-1)^n}{2n^2} \left(x - 1 + \sum_{s=2}^n c_n^{(s)} \frac{x^s - x}{s - 1} \right), \quad (2.19)$$

which gives a polynomial approximation of $y(x) = x \ln x$ [21]. Since it oscillates around the function to be fitted, we will further use a modification of (2.19). Indeed, the polynomial (2.19) does not vanish at the point $x = 0$. For odd n , it takes the value $1/(2n^2) > 0$ for $x = 0$, whereas the original function is negative for all $x \in (0, 1)$. The constant term in (2.19) is determined by the choice of $T_n^*(x)$ on the right, and any term $\propto x$ is a solution of homogeneous equation. Adding to (2.19) the linear term $(-1)^n(1 - x)/(2n^2)$, for $n \geq 2$ we finally write

$$g_n(x) = \frac{(-1)^n}{2n^2} \sum_{s=2}^n c_n^{(s)} \frac{x^s - x}{s - 1}, \quad (2.20)$$

so that $g_n(0) = 0$ and $g_n(1) = 0$. Polynomials of the form (2.20) are the first main finding of this work. It turns out that they provide approximation of $y(x)$ from above.

Let us consider values of the first derivative at the least points of the interval $x \in [0, 1]$. It follows from (B1) that $g'_n(1) = 1$ for even $n \geq 2$ and

$$g'_n(1) = 1 - \frac{1}{n^2} \quad (2.21)$$

for odd $n \geq 3$. The value of $g'_n(0)$ is more difficult to write an expression with definite sign. In Appendix B, we obtain (B7), whence the following sums are derived:

$$g'_n(0) = -\frac{4}{n^2} \sum_{r=1}^{\lfloor n/2 \rfloor} \frac{4r^2}{n - 2r} \quad (n \text{ odd}), \quad (2.22)$$

$$g'_n(0) = -\frac{4}{n^2} \sum_{r=1}^{\lfloor n/2 \rfloor} \frac{(2r - 1)^2}{n - 2r + 1} \quad (n \text{ even}). \quad (2.23)$$

We shall now compare the first derivatives of $g_n(x)$ and $y(x)$ at the least points of the range $x \in [0, 1]$.

To approximate the original function, the graph of $g_n(x)$ should go closely to the graph of $y(x)$. Since $y'(x) = 1 + \ln x \rightarrow -\infty$ for $x \rightarrow +0$, near $x = 0$ the graph of $y(x)$ comes to the horizontal axis from negative values with almost vertical slope. Hence, the value $g'_n(0)$ is expected to be negative. On the other hand, this value is certainly finite, so that the slope of tangential line is somehow far from the vertical. Therefore, in some right neighborhood of the point $x = 0$ our approximation have to be relatively poor. But, derivatives are inevitably finite for any polynomial. Nevertheless, the absolute value of $g'_n(0)$ increases with growth of n , so our approximation becomes better. It follows from $-\infty < g'_n(0) < 0$ and $g_n(0) = y(0)$ that $g_n(x)$ exceeds $y(x)$ in some right neighborhood of the point $x = 0$. In

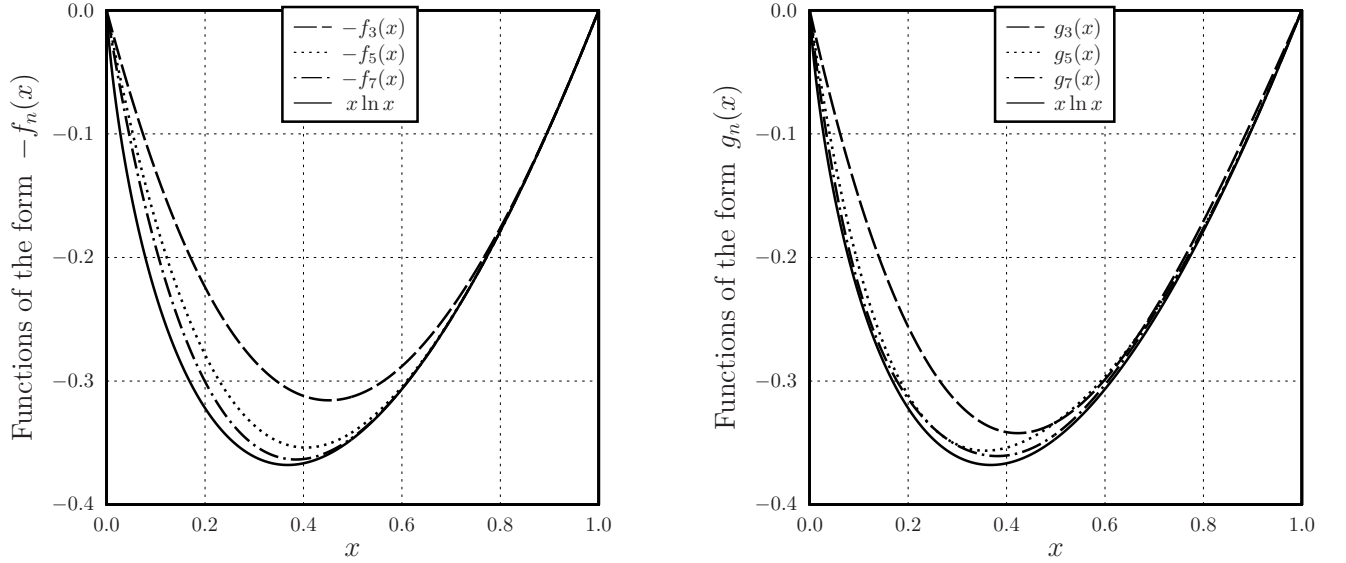


FIG. 1: Several functions to approximate $x \ln x$ for $n = 3, 5, 7$. The left plot shows minus (2.13) and the right one shows (2.20).

Appendix B, we obtain explicit expressions for $g_n''(x)$ for $2 \leq n \leq 15$, whence convexity is seen. Therefore, the graph of $g_n(x)$ goes over the graph of the function $x \mapsto g_n'(0)x$. For $n \geq 2$, the inequality

$$x \ln x \leq g_n(x) \quad (2.24)$$

holds at least for $0 \leq x \leq \exp(g_n'(0))$. The latter is small for sufficiently large values of n .

Combining $g_n(1) = y(1)$ and $y'(1) = 1$ with (2.21) shows the following. For odd $n \geq 3$, we have (2.24) in a left neighborhood of the point $x = 1$, since

$$g_n(x) - y(x) = \frac{1-x}{n^2} + O((x-1)^2). \quad (2.25)$$

For even $n \geq 2$, the first derivatives are equal, i.e., $g_n'(1) = y'(1)$. It follows from the results of Appendix B that $g_n''(1) = 0$ for odd n and $g_n''(1) = 2$ for even $n \geq 2$. Combining this with $y''(1) = 1$, we compare the functions of interest up to the terms quadratic in $(x-1)$. Namely, it holds for even $n \geq 2$ that

$$g_n(x) - y(x) = (x-1)^2 + O((x-1)^3). \quad (2.26)$$

For even n , herewith, the inequality (2.24) holds at least near the point $x = 1$.

Let us summarize the above observation. In points of the range $x \in [0, 1]$ sufficiently close to one of the least points we have the result (2.24). For intermediate points of the interval, the validity of (2.24) can be checked numerically. In effect, for such points the difference $g_n(x) - y(x)$ does not take vanishing values. Unfortunately, analytical reasons to justify (2.24) for all $x \in [0, 1]$ are still not found. In addition, coefficients $c_n^{(s)}$ increase considerably with growth of n . For these reasons, we will restrict a consideration for values of n up to $n = 15$. With $n = 15$, the difference between the sides of (2.24) is less than one thousandth of the maximum of $|x \ln x|$ in the interval $x \in [0, 1]$. Hence, further increasing of n cannot lead to any noticeable improvements of accuracy. To visualize the observations made, we draw $y(x)$, $-f_n(x)$ and $g_n(x)$ versus $x \in [0, 1]$ for $n = 3, 5, 7$ in Fig. 1. We have chosen these values, since examples of quantum designs for $t = 3, 5, 7$ will be discussed in the next section. At fixed n , curves of the right box improve approximation for relatively small x without introducing considerable errors in a left vicinity of the point $x = 1$. For $n = 3$, that both the estimates are not very good in comparison with other estimates.

Now, we are in position to formulate another two-sided estimate on the Shannon entropy. The following estimate from below takes place due to (2.24):

$$\sum_{s=1}^n \tilde{a}_n^{(s)} x^s \leq -x \ln x. \quad (2.27)$$

Here, the coefficients are expressed in terms of coefficients of n -th Chebyshev polynomial by the formulas

$$\tilde{a}_n^{(1)} = \frac{(-1)^n}{2n^2} \sum_{s=2}^n \frac{c_n^{(s)}}{s-1}, \quad \tilde{a}_n^{(s)} = \frac{(-1)^{n+1}}{2n^2} \frac{c_n^{(s)}}{s-1} \quad (2 \leq s \leq n). \quad (2.28)$$

For $n = 2$, the left-hand side of (2.27) is equal to $f_2(x) = x - x^2$. It is not the case for $n \geq 3$. Applying (2.6) and (2.9) with $g_n(x)$ finally leads to

$$-x \ln x \leq \tilde{b}_n^{(0)} + \sum_{s=1}^n \tilde{b}_n^{(s)} x^s, \quad (2.29)$$

where

$$\tilde{b}_n^{(0)} = 1 - \sum_{s=1}^n \frac{\tilde{a}_n^{(s)}}{s}, \quad \tilde{b}_n^{(1)} = \tilde{a}_n^{(1)} - 1, \quad \tilde{b}_n^{(s)} = \frac{\tilde{a}_n^{(s)}}{s} \quad (2 \leq s \leq n). \quad (2.30)$$

The result (2.29) allows us to estimate the Shannon entropy from above. For $n = 2$, the inequality (2.29) coincides with (2.15). For other values of n , coefficients of polynomials in the formulas (2.27) and (2.29) do not correspond to the Taylor scheme. Hence, the estimates by means of (2.27) and (2.29) are not very good near the point $x = 1$. For points sufficiently close to 1 from the left, we prefer (2.15) and (2.15). In regions peripheral to $x = 1$, the results (2.27) and (2.29) provide more accurate estimation. This distinction is especially clear near the point $x = 0$. Nevertheless, any estimate by polynomials will hardly be very precise for points close to 0 from the right. In effect, the function of interest is not analytic in this point.

Thus, there is an asymmetry in estimating the function $x \mapsto -x \ln x$ in regions close respectively to one of the two least points of the range $x \in [0, 1]$. It is also validated by some numerical inspection. To make estimates better, one shall move actual points of approximation to the right, where expected errors are lesser. It can be made if we can estimate the maximal probability from above. When the sum of integer powers of probabilities is known exactly, this question was solved in [17]. The answer follows from consideration of equation of the corresponding oval line. Suppose that L probabilities p_j obey

$$\sum_{j=1}^L p_j^n = I^{(n)} \quad (2.31)$$

for integer $n \geq 2$. It then holds that [17]

$$\max_j p_j \leq \Upsilon_{L-1}^{(n)}(I^{(n)}), \quad (2.32)$$

where $\Upsilon_{K-1}^{(n)}(I^{(n)})$ denotes the maximal real root of the algebraic equation

$$(1 - \Upsilon)^n + (L - 1)^{n-1} \Upsilon^n = (L - 1)^{n-1} I^{(n)}. \quad (2.33)$$

When other parameters are fixed, the quantity $\Upsilon_{L-1}^{(n)}(I^{(n)})$ is increasing and concave with respect to $I^{(n)}$ [17].

For $n \geq 5$, we are generally unable to write $\Upsilon_{L-1}^{(n)}(I^{(n)})$ analytically using radicals. On the other hand, for the given parameters the result can always be calculated by appropriate numerical procedure with any desired accuracy. For $n = 2, 3, 4$, one can express the answer in a closed analytic form. In particular, the case $n = 2$ is answered by

$$\Upsilon_{L-1}^{(2)}(I^{(2)}) = \frac{1}{L} \left(1 + \sqrt{L-1} \sqrt{L I^{(2)} - 1} \right). \quad (2.34)$$

This result was presented and applied to entropic uncertainty relations in the paper [22]. Due to our findings, the following statement takes place.

Proposition 1 *Let $I^{(s)}(\mathbf{p})$ be given for all $s = 2, \dots, n$. Then the Shannon entropy satisfies*

$$\sum_{s=1}^n a_n^{(s)} \Upsilon^{1-s} I^{(s)}(\mathbf{p}) - \ln \Upsilon \leq H_1(\mathbf{p}) \leq \frac{\Upsilon L}{n} + \sum_{s=1}^n b_n^{(s)} \Upsilon^{1-s} I^{(s)}(\mathbf{p}) - \ln \Upsilon, \quad (2.35)$$

where $\Upsilon = \Upsilon_{L-1}^{(n)}(I^{(n)})$ and the coefficients $a_n^{(s)}$ and $b_n^{(s)}$ are defined by (2.14) and (2.17), respectively. It also holds that

$$\sum_{s=1}^{\tilde{n}} \tilde{a}_{\tilde{n}}^{(s)} \Upsilon^{1-s} I^{(s)}(\mathbf{p}) - \ln \Upsilon \leq H_1(\mathbf{p}) \leq \tilde{b}_{\tilde{n}}^{(0)} \Upsilon L + \sum_{s=1}^{\tilde{n}} \tilde{b}_{\tilde{n}}^{(s)} \Upsilon^{1-s} I^{(s)}(\mathbf{p}) - \ln \Upsilon, \quad (2.36)$$

where $\tilde{n} = \min\{n, 15\}$ and the coefficients are defined by (2.28) and (2.30).

Proof. Let us define the points of approximation $x_j = p_j/\Upsilon$. Due to (2.32), they all lie in the interval $x \in [0, 1]$. Substituting $p_j = \Upsilon x_j$ into (2.1) results in the expression

$$H_1(\mathbf{p}) = -\ln \Upsilon - \Upsilon \sum_{j=1}^L x_j \ln x_j. \quad (2.37)$$

Using (2.12) and (2.15) in all the points x_j , we obtain after summation that

$$\sum_{s=1}^n a_n^{(s)} \frac{I^{(s)}(\mathbf{p})}{\Upsilon^s} \leq -\sum_{j=1}^L x_j \ln x_j \leq \frac{L}{n} + \sum_{s=1}^n b_n^{(s)} \frac{I^{(s)}(\mathbf{p})}{\Upsilon^s}. \quad (2.38)$$

Combining (2.37) with (2.38) completes the proof of (2.35). In a similar manner, the two-sided estimate (2.36) follows from (2.27) and (2.29). The only additional point is that we restrict an application of (2.27) and (2.29) by values $n \leq 15$. ■

The statement of Proposition 1 provides two-sided estimates on the Shannon entropy, when several indices of the form (2.4) are given exactly. It is natural to ask how good are the presented estimates. We prefer to examine this principal question within applications to concrete examples. In the next section, we will use (2.35) and (2.36) to derive uncertainty and certainty relations for POVMs assigned to a quantum design. Quantum designs they are an interesting object even from purely mathematical viewpoint. Recently, quantum designs have found a lot of attention due to potential applications in quantum information processing. Finally, we formulate an interesting inequality between the Shannon entropy and Tsallis entropies of integer degree $s \geq 2$. We conjecture that

$$H_1(\mathbf{p}) \geq \frac{(-1)^n}{2n^2} \sum_{s=2}^n c_n^{(s)} H_s(\mathbf{p}), \quad (2.39)$$

where $c_n^{(s)}$ denotes the corresponding coefficient of n -th shifted Chebyshev polynomial. Explicitly, these coefficients are written in (A4). The conjectured inequality follows from (2.24) and holds at least up to $n = 15$. The latter restriction was chosen rather for convenience in practical calculations. Checking the validity of (2.39) for arbitrary natural n remains an open question. Especially, some proof by analytical tools would be desired.

III. UNCERTAINTY AND CERTAINTY RELATIONS FOR DESIGN-STRUCTURED POVMS

This section is devoted to complementarity relations for POVMs assigned to a quantum design. When several indices of the form (2.4) are given, uncertainty and certainty relations directly follow from the results of the previous section. Let us recall briefly the required material concerning quantum designs. Dealing with rays in d -dimensional Hilbert space, one selects K unit vectors $|\phi_k\rangle$ with the following property. For all real polynomials \mathcal{P}_t of degree at most t it holds that [14]

$$\frac{1}{K^2} \sum_{j,k=1}^K \mathcal{P}_t(|\langle \phi_j | \phi_k \rangle|^2) = \int \int d\mu(\psi) d\mu(\psi') \mathcal{P}_t(|\langle \psi | \psi' \rangle|^2). \quad (3.1)$$

By $\mu(\psi)$, one denotes the unique unitarily-invariant probability measure on the corresponding complex projective space induced by the Haar measure. Then unit vectors $|\phi_k\rangle$ are said to form a quantum t -design. Quantum designs have interesting formal properties. Let $\Pi_{\text{sym}}^{(t)}$ be the projector onto the symmetric subspace of $\mathcal{H}^{\otimes t}$. The trace of $\Pi_{\text{sym}}^{(t)}$ gives dimensionality of the symmetric subspace. It holds that [14]

$$\frac{1}{K} \sum_{k=1}^K |\phi_k\rangle \langle \phi_k|^{\otimes t} = \mathcal{D}_d^{(t)} \Pi_{\text{sym}}^{(t)}, \quad (3.2)$$

where $\mathcal{D}_d^{(t)}$ denotes the inverse of $\text{tr}(\Pi_{\text{sym}}^{(t)})$, namely

$$\mathcal{D}_d^{(t)} = \binom{d+t-1}{t}^{-1} = \frac{t!(d-1)!}{(d+t-1)!}. \quad (3.3)$$

At the given t , we can rewrite (3.2) for all positive integers $s \leq t$. Substituting $s = 1$ leads to the formula

$$\frac{d}{K} \sum_{k=1}^K |\phi_k\rangle\langle\phi_k| = \mathbb{1}_d. \quad (3.4)$$

Thus, unit vectors $|\phi_k\rangle$ allow us to build to a resolution of the identity in \mathcal{H} . In principle, there may be several resolutions assigned to the given t -design. We cannot list all of them *a priori*, without an explicit analysis of $|\phi_k\rangle$. Obviously, one can take the complete set \mathcal{E} consisting of operators

$$\mathbf{E}_k = \frac{d}{K} |\phi_k\rangle\langle\phi_k|. \quad (3.5)$$

Sometimes, M rank-one POVMs $\{\mathcal{E}^{(m)}\}_{m=1}^M$ can be assigned to the given quantum design. Each of these POVMs consists of ℓ operators of the form

$$\mathbf{E}_j^{(m)} = \frac{d}{\ell} |\phi_j^{(m)}\rangle\langle\phi_j^{(m)}|. \quad (3.6)$$

The integers ℓ and M are connected by $K = \ell M$.

If the state of interest is described by density matrix $\boldsymbol{\rho}$, then the probability of j -th outcome is equal to

$$p_j(\mathcal{E}^{(m)}; \boldsymbol{\rho}) = \frac{d}{\ell} \langle\phi_j^{(m)}|\boldsymbol{\rho}|\phi_j^{(m)}\rangle. \quad (3.7)$$

Substituting these probabilities into (2.1) gives the entropy $H_1(\mathcal{E}^{(m)}; \boldsymbol{\rho})$. It follows from (3.2) that [16]

$$\frac{1}{K} \sum_{k=1}^K \langle\phi_k|\boldsymbol{\rho}|\phi_k\rangle^s = \mathcal{D}_d^{(s)} \text{tr}(\boldsymbol{\rho}^{\otimes s} \Pi_{\text{sym}}^{(s)}). \quad (3.8)$$

Combining (3.7) with (3.8) then gives

$$\sum_{m=1}^M \sum_{j=1}^{\ell} p_j(\mathcal{E}^{(m)}; \boldsymbol{\rho})^s = \left(\frac{d}{n}\right)^t \sum_{k=1}^K \langle\phi_k|\boldsymbol{\rho}|\phi_k\rangle^t = K \ell^{-s} d^s \mathcal{D}_d^{(s)} \text{tr}(\boldsymbol{\rho}^{\otimes s} \Pi_{\text{sym}}^{(s)}), \quad (3.9)$$

where $s = 2, \dots, t$. When a single POVM is assigned, one has $\ell = K$ and

$$\sum_{k=1}^K p_k(\mathcal{E}; \boldsymbol{\rho})^s = K^{1-s} d^s \mathcal{D}_d^{(s)} \text{tr}(\boldsymbol{\rho}^{\otimes s} \Pi_{\text{sym}}^{(s)}). \quad (3.10)$$

The results (3.9) and (3.10) remains valid with $s = 2, \dots, t$ instead of t . The authors of [16, 23] resolved the question how to express $\text{tr}(\boldsymbol{\rho}^{\otimes t} \Pi_{\text{sym}}^{(t)})$ as a sum of monomials of the moments of $\boldsymbol{\rho}$. Of course, complexity of such expressions increases with growth of t . To avoid bulky expressions in the following, we introduce the two quantities

$$\bar{\beta}_{\ell}^{(s)}(\boldsymbol{\rho}) = \ell^{1-s} d^s \mathcal{D}_d^{(s)} \text{tr}(\boldsymbol{\rho}^{\otimes s} \Pi_{\text{sym}}^{(s)}), \quad (3.11)$$

$$\bar{\beta}^{(s)}(\boldsymbol{\rho}) = K^{1-s} d^s \mathcal{D}_d^{(s)} \text{tr}(\boldsymbol{\rho}^{\otimes s} \Pi_{\text{sym}}^{(s)}), \quad (3.12)$$

where $s = 2, \dots, t$. The term (3.12) is obtained from (3.11) for $\ell = K$. For a pure state $\boldsymbol{\rho} = |\psi\rangle\langle\psi|$, the trace in (3.11) is equal to 1, so that

$$\bar{\beta}_{\ell}^{(s)}(|\psi\rangle\langle\psi|) = \ell^{1-s} d^s \mathcal{D}_d^{(s)}. \quad (3.13)$$

The formulas (3.9) and (3.10) allow us to derive entropic uncertainty relations for design-structured POVMs. Uncertainty relations in terms of generalized entropies were considered in [16, 17]. Findings of the previous section allow one to obtain uncertainty and certainty relations in terms of the Shannon entropy. The relations are posed as follows.

Proposition 2 *Let M rank-one POVMs $\mathcal{E}^{(m)}$, each with ℓ elements of the form (3.6), be assigned to a quantum t -design $\mathbb{D} = \{|\phi_k\rangle\}_{k=1}^K$ in d dimensions. It then holds that*

$$\sum_{s=1}^t a_t^{(s)} \Upsilon^{1-s} \bar{\beta}_{\ell}^{(s)}(\boldsymbol{\rho}) - \ln \Upsilon \leq \frac{1}{M} \sum_{m=1}^M H_1(\mathcal{E}^{(m)}; \boldsymbol{\rho}) \leq \frac{\Upsilon \ell}{t} + \sum_{s=1}^t b_t^{(s)} \Upsilon^{1-s} \bar{\beta}_{\ell}^{(s)}(\boldsymbol{\rho}) - \ln \Upsilon, \quad (3.14)$$

where $\Upsilon = \min\{M \Upsilon_{K-1}^{(t)}(\bar{\beta}^{(t)}(\rho)), 1\}$. For $n = \min\{t, 15\}$, it holds that

$$\sum_{s=1}^n \tilde{a}_n^{(s)} \Upsilon^{1-s} \bar{\beta}_\ell^{(s)}(\rho) - \ln \Upsilon \leq \frac{1}{M} \sum_{m=1}^M H_1(\mathcal{E}^{(m)}; \rho) \leq \tilde{b}_n^{(0)} \Upsilon \ell + \sum_{s=1}^n \tilde{b}_n^{(s)} \Upsilon^{1-s} \bar{\beta}_\ell^{(s)}(\rho) - \ln \Upsilon. \quad (3.15)$$

Proof. For the case of M POVMs, the left-hand side of (3.9) is actually the sum of s -indices for all POVMs. For all $k = 1, \dots, K$, one has

$$\frac{d}{K} \langle \phi_k | \rho | \phi_k \rangle = p_k(\mathcal{E}; \rho) \leq \Upsilon_{K-1}^{(t)}(\bar{\beta}^{(t)}(\rho))$$

whence

$$\frac{d}{\ell} \langle \phi_j^{(m)} | \rho | \phi_j^{(m)} \rangle = p_j(\mathcal{E}^{(m)}; \rho) \leq M \Upsilon_{K-1}^{(t)}(\bar{\beta}^{(t)}(\rho)) \quad (3.16)$$

due to $K = \ell M$. To each of M entropies $H_1(\mathcal{E}^{(m)}; \rho)$, we apply the two-sided estimate (2.35) with maximal power t and the defined Υ , so that

$$\sum_{s=1}^t a_t^{(s)} \Upsilon^{1-s} I^{(s)}(\mathbf{p}^{(m)}) - \ln \Upsilon \leq H_1(\mathcal{E}^{(m)}; \rho) \leq \frac{\Upsilon \ell}{n} + \sum_{s=1}^t b_t^{(s)} \Upsilon^{1-s} I^{(s)}(\mathbf{p}^{(m)}) - \ln \Upsilon. \quad (3.17)$$

It is seen from (3.9) that, for all $s = 2, \dots, t$,

$$\sum_{m=1}^M I^{(s)}(\mathbf{p}^{(m)}) = K \ell^{-s} d^s \mathcal{D}_d^{(s)} \text{tr}(\rho^{\otimes s} \Pi_{\text{sym}}^{(s)}) = M \bar{\beta}_\ell^{(s)}(\rho). \quad (3.18)$$

Summing (3.17) with respect to m and substituting (3.18), we get (3.14) multiplied by common factor M . Similar reasons allow us to derive (3.15) from (2.36). We only restrict a consideration to $n = \min\{t, 15\}$. ■

Thus, we have obtained two families of complementarity relations for the Shannon entropy averaged over all M POVMs $\mathcal{E}^{(m)}$. When single POVM \mathcal{E} with K elements (3.5) is assigned to the given t -design, the relations (3.14) and (3.15) respectively reduce to

$$\sum_{s=1}^t a_t^{(s)} \Upsilon^{1-s} \bar{\beta}^{(s)}(\rho) - \ln \Upsilon \leq H_1(\mathcal{E}; \rho) \leq \frac{\Upsilon K}{t} + \sum_{s=1}^t b_t^{(s)} \Upsilon^{1-s} \bar{\beta}^{(s)}(\rho) - \ln \Upsilon, \quad (3.19)$$

$$\sum_{s=1}^n \tilde{a}_n^{(s)} \Upsilon^{1-s} \bar{\beta}^{(s)}(\rho) - \ln \Upsilon \leq H_1(\mathcal{E}; \rho) \leq \tilde{b}_n^{(0)} \Upsilon K + \sum_{s=1}^n \tilde{b}_n^{(s)} \Upsilon^{1-s} \bar{\beta}^{(s)}(\rho) - \ln \Upsilon. \quad (3.20)$$

We shall below consider several examples concerning mainly (3.19) and (3.20). They are a reflection of sufficiently strong restrictions imposed on measurement statistics for design-structured POVMs. Hence, complementarity relations for various entropic functions follow. Uncertainty relations in terms of generalized entropies were considered in [16, 17]. In a sense, the above discussion complements the analysis by adding relations in terms of the Shannon entropy. For a pure state, the left-hand sides of (3.14) and (3.15) read as

$$\frac{1}{M} \sum_{m=1}^M H_1(\mathcal{E}^{(m)}; |\psi\rangle\langle\psi|) \geq \sum_{s=1}^t a_t^{(s)} \Upsilon^{1-s} \ell^{1-s} d^s \mathcal{D}_d^{(s)} - \ln \Upsilon, \quad (3.21)$$

$$\frac{1}{M} \sum_{m=1}^M H_1(\mathcal{E}^{(m)}; |\psi\rangle\langle\psi|) \geq \sum_{s=1}^n \tilde{a}_n^{(s)} \Upsilon^{1-s} \ell^{1-s} d^s \mathcal{D}_d^{(s)} - \ln \Upsilon, \quad (3.22)$$

where $\Upsilon = \min\{M \Upsilon_{K-1}^{(t)}(K^{1-t} d^t \mathcal{D}_d^{(t)}), 1\}$. The following fact about (3.21) and (3.22) will further be seen with concrete examples of quantum designs. The lower entropic bounds obtained for pure states remain valid for all states. This conclusion is natural, but its validity is not easy to prove analytically. However, we can always check the mentioned fact by numerical inspection in each concrete example of design-structured POVMs. If so, the right-hand sides of (3.21) and (3.22) give a state-independent formulation of uncertainty relations. Of course, the state-independent upper bound is merely $\ln \ell$ for the case of M POVMs and $\ln K$ for the case of single POVM.

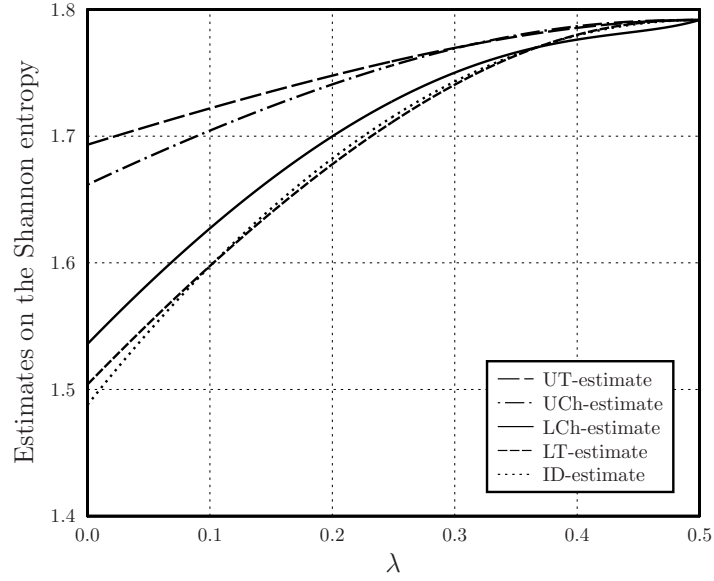


FIG. 2: Estimates on the Shannon entropy versus λ for the 3-design with 6 vertices.

Let us compare the above finding with relations previously published in the literature. Here, we quote some results of the papers [3, 24]. One of the results of Harremoës and Topsøe [3] can be reformulated as follows [24]. For probability distribution \mathbf{p} with K probabilities, it holds that

$$H_1(\mathbf{p}) \geq \ln(k+1) + k \ln\left(\frac{k+1}{k}\right) - k(k+1) \ln\left(\frac{k+1}{k}\right) I(\mathbf{p}) \quad (1 \leq k \leq K-1), \quad (3.23)$$

where k should be integer. To get optimal lower bound from (3.23), we take k depending on the actual value of $I(\mathbf{p})$. For the sake of simplicity of presentation, we further use the right-hand side of the inequality

$$H_1(\mathbf{p}) \geq \ln K + (K-1) \ln\left(\frac{K}{K-1}\right) - K(K-1) \ln\left(\frac{K}{K-1}\right) I(\mathbf{p}), \quad (3.24)$$

which is optimal for states close to the maximally mixed one. For pure states and states with low mixedness, the choice $k = K - 1$ is not optimal. On the other hand, selecting a suitable value of k results here in changes within few percents. Since we will use estimates from information diagrams only as a reference point, the inequality (3.24) is suitable.

Let us proceed to examples of applications to concrete quantum designs in two dimensions. A short description of these designs in terms of components of the Bloch vector are given in [16]. This vector comes to one of vertices forming some polyhedron. To characterize the qubit density matrix, its minimal eigenvalue λ is used. It is instructive to visualize the two-sided estimates (3.14) and (3.15) together with (3.24). To avoid bulky legends on figures, the following notation will be utilized. By “LT-estimate” and “UT-estimate”, we mean the left- and right-hand sides of (3.14), respectively. They are based on approximation by polynomials, whose coefficients are due to the Taylor scheme. The terms “LCh-estimate” and “UCh-estimate” respectively refer to the left- and right-hand sides of (3.15). Due to (2.24), such estimates use polynomials with coefficients linked to coefficients of the shifted Chebyshev polynomials. The right-hand side of (3.24) following from information diagrams will be referred to as “ID-estimate”. We will mainly focus on the case of single assigned POVM.

Let us begin with the 3-design with $K = 6$ vertices forming octahedron. In Fig. 2, we plot the three lower estimates and the two upper ones as functions of λ . Of course, the corresponding Shannon entropy varies in sufficiently restricted diapason. The two-sided estimate (3.19) is better only for states close to the maximally mixed one. It turned out in this example that the left-hand side of (3.19) is almost coinciding with the lower estimate obtained from information diagrams. The formula (3.20) shows considerably better results for pure states and states with low mixedness. For pure states, the difference between LCh-estimate and ID-estimate is more then one third of the difference between UCh-estimate and LCh-estimate. The latter point is characterized by one fifth with selecting $k = 2$ in (3.23), when ID-estimate slightly improved for pure states. For states with low mixedness, the left-hand side of (3.20) provides much stronger uncertainty bound. For the maximally mixed state, the five curves are all converging at one point.

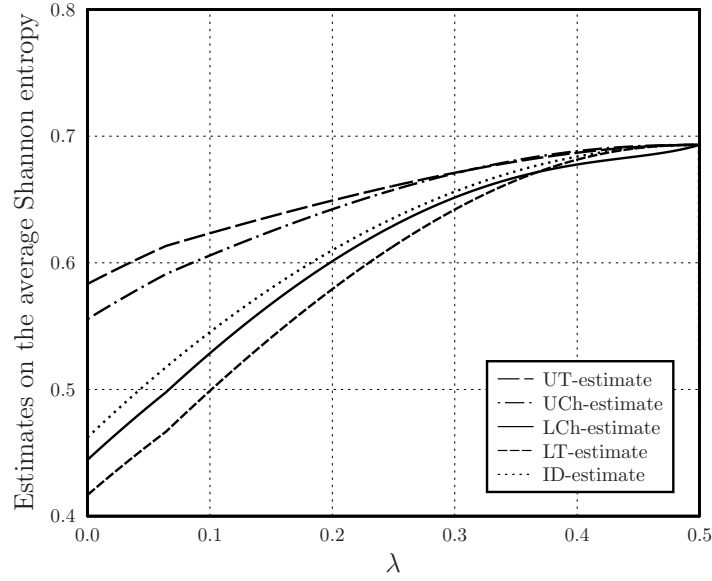


FIG. 3: Estimates on the average Shannon entropy versus λ for the three mutually unbiased bases in two dimensions.

The example with octahedron is also interesting due to the fact that the 3-design of interest is formed by eigenstates of the Pauli matrices. That is, we deal the complete set of three mutually unbiased bases in two dimensions. Entropic uncertainty relations for such bases were extensively examined for several reasons. Using (3.25), the authors of [24] studied entropic uncertainty relations for a set mutually unbiased bases. For $M = 3$ and $d = 2$, their main result reads as

$$\frac{1}{3} \sum_{m=1}^3 H_1(\mathcal{E}^{(m)}; \rho) \geq \frac{2 - \text{tr}(\rho^2)}{3} \ln 4. \quad (3.25)$$

In this example, the right-hand side of (3.25) will be referred to as ID-estimate. The five estimates on the average Shannon entropy are presented in Fig. 3. In this example, ID-estimate provides better lower bound. For pure states, the difference between ID-estimate and LCh-estimate is almost one fifth the difference between UCh-estimate and ID-estimate. Commenting Fig. 1, we already noticed that our estimates are not very good for $n = 3$. Another origin for comparatively poor results of (3.15) is connected with a behavior of Υ . Indeed, one has $3\Upsilon_5^{(t)}(\bar{\beta}^{(3)}(\rho)) > 1$ for states with sufficiently low mixedness. It was shown in [17] that the average maximal entropy obeys

$$\frac{1}{M} \sum_{m=1}^M \max_j p_j(\mathcal{E}^{(m)}; \rho) \leq \Upsilon_{\ell-1}^{(t)}(\bar{\beta}_{\ell}^{(t)}(\rho)). \quad (3.26)$$

Substituting $t = 3$ and $\ell = 2$, the right-hand side of (3.26) is much tighter for states with moderate mixedness. Methods of deriving (3.14) and (3.15) are such that one can hardly be able to use just (3.26). The right-hand side of (3.23) has much simpler analytical structure, so that results of the form (3.25) follow. This example shows that our two-sided estimates provide better results in application to a single entropy. As was already mentioned, only the sum of s -indices up to $s = t$ is given by (3.9).

The following example is the 5-design with $K = 12$ vertices forming an icosahedron. The three lower bounds and two upper bounds versus λ are shown in Fig. 4. Of course, allowed changes of the corresponding Shannon entropy are enough limited in their value. Again, the two-sided estimate (3.19) is better only for states sufficiently close to the maximally mixed one. On the other hand, we see wider region in which the result (3.19) leads to stronger bounds. For states with low mixedness, the left-hand sides of (3.19) and (3.20) are both considerably stronger than the lower estimate obtained from the information diagrams. For pure states, the difference between LCh-estimate and ID-estimate is almost twice the difference between UCh-estimate and LCh-estimate. In other words, ID-estimate is here far from actual entropic values. We could expect this, since it is based on the index of coincidence (2.3), whereas other estimates take into account five indices of the form (2.4). Similarly to the previous examples, all the five curves converge at one point for the maximally mixed state.

Let us consider also the 5-design with $K = 30$ vertices forming an icosidodecahedron. On the average, allowed values of the Shannon entropy are larger in view of increased number of outcomes. The five curves shown in Fig. 5 curves

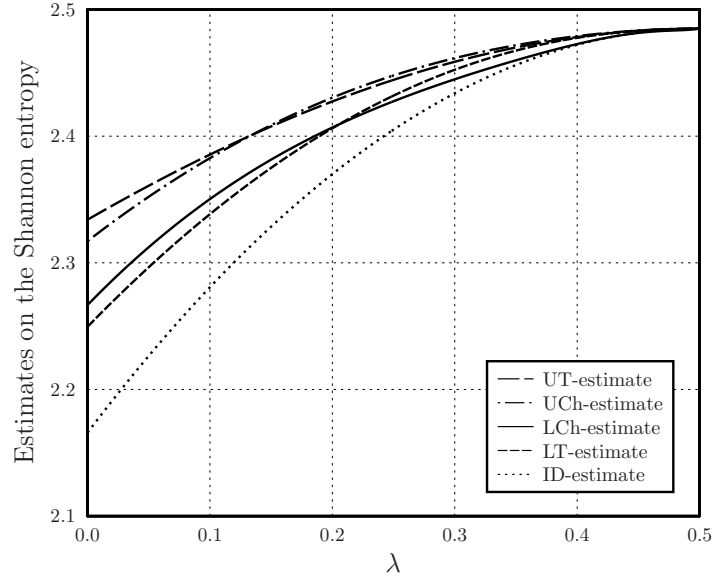


FIG. 4: Estimates on the Shannon entropy versus λ for the 5-design with 12 vertices.

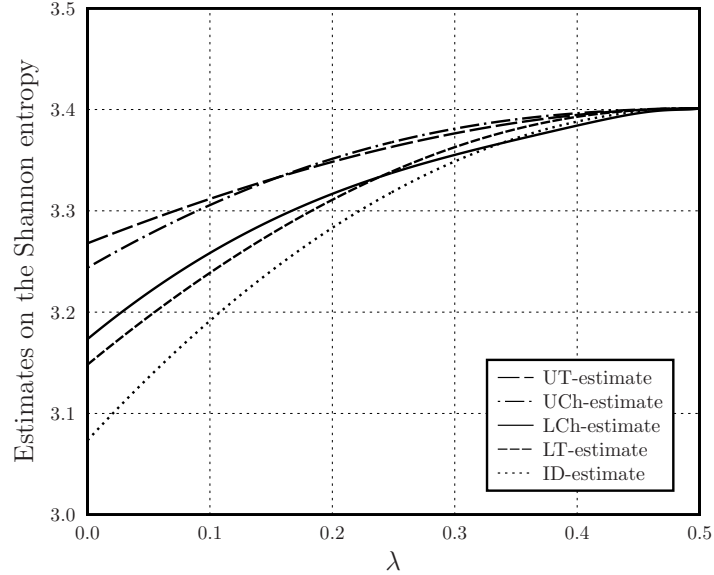


FIG. 5: Estimates on the Shannon entropy versus λ for the 5-design with 30 vertices.

form a picture quite similarly to the previous example. The interval $\lambda \in [0, 1/2]$ is divided into two approximately equal parts. The former is where the two-sided estimate (3.20) gives better results, and the latter is a domain for the use of (3.19). As before, for pure states ID-estimate is sufficiently far from optimality. In effect, the difference between LCh-estimate and ID-estimate is almost one and a half times greater than the difference between UCh-estimate and LCh-estimate. Nevertheless, this distinction is less than in the previous case with 12 vertices. Closely to the mixed states, all the five curves become coinciding. Other behavior would indicate an insufficiency of estimates.

Finally, we test the discussed estimates with the 7-design obtained from a deformed snub cube. The regular snub cube has 60 equal edges, and its 24 vertices form a 3-design [25]. Moving these vertices slightly, one can obtain a 7-design. In detail, this step is described in [25]. The resulting 7-design was first found by McLaren [26]. In Fig. 6, we plot the estimates of interest for the McLaren design. A range for possible values of the Shannon entropy is more narrow than in the previous examples. Another consequence of increasing t is that ID-estimate becomes insufficient for states of low mixedness. Now, the difference between LCh-estimate and ID-estimate more than 4 times exceeds the difference between UCh-estimate and LCh-estimate. Again, all five curves tend to coincide closely to the maximally

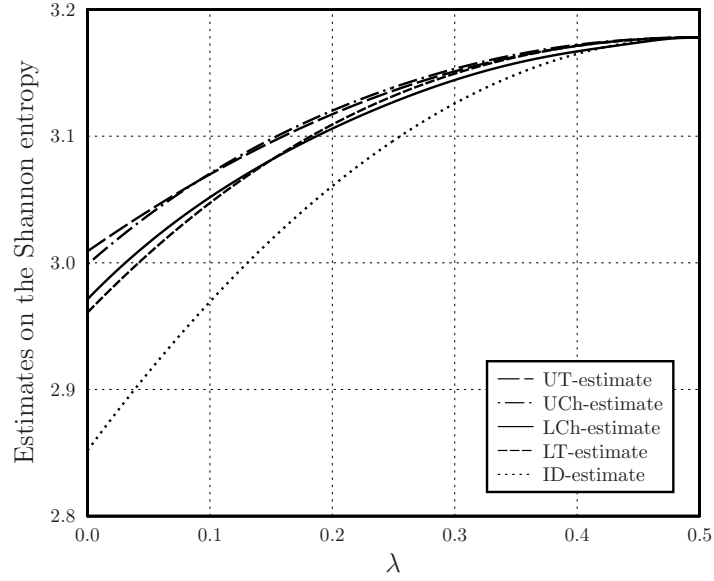


FIG. 6: Estimates on the Shannon entropy versus λ for the 7-design with 24 vertices.

mixed state. The two-sided estimate (3.20) gives better results for states with low mixedness. For sufficiently mixed states, the two-sided estimate (3.19) is preferable. At the same time, distinctions between these estimates are less than in the previous examples.

Design-structured POVM can be used for estimating the von Neumann entropy of quantum state, when enough number of its copies are available for observations. Recall that the von Neumann entropy is defined as

$$H_1(\rho) := -\text{tr}(\rho \ln \rho). \quad (3.27)$$

Using quantities of the form (3.11) or (3.12), one can recalculate the traces $\text{tr}(\rho^s)$ for $s = 2, \dots, t$. We restrict a consideration to the case of single assigned POVM. Note that the right-hand side of (3.27) can be interpreted as the Shannon entropy calculated with the eigenvalues of ρ . Adapting (2.35) and (2.36) to this case, one has

$$\sum_{s=1}^t a_t^{(s)} \Lambda^{1-s} \text{tr}(\rho^s) - \ln \Lambda \leq H_1(\rho) \leq \frac{\Lambda d}{t} + \sum_{s=1}^t b_t^{(s)} \Lambda^{1-s} \text{tr}(\rho^s) - \ln \Lambda, \quad (3.28)$$

$$\sum_{s=1}^n \tilde{a}_n^{(s)} \Lambda^{1-s} \text{tr}(\rho^s) - \ln \Lambda \leq H_1(\rho) \leq \tilde{b}_n^{(0)} \Lambda d + \sum_{s=1}^n \tilde{b}_n^{(s)} \Lambda^{1-s} \text{tr}(\rho^s) - \ln \Lambda, \quad (3.29)$$

where $\Lambda = \Upsilon_{d-1}^{(t)}(\text{tr}(\rho^t))$ and $n = \min\{t, 15\}$. Here, the quantity Λ estimates the eigenvalues of ρ from above. The two-sided estimates (3.28) and (3.29) could be useful in questions of quantum tomography.

The above uncertainty relations for design-structured POVMs can be used to formulate quantum steering inequalities. This question was already addressed in [16, 17]. So, we will discuss steering inequalities very shortly. The phenomenon of steering initially noticed by Schrödinger was rigorously formalized in [27]. In detail, quantum steering and its applications are reviewed in [28]. Alice and Bob share a bipartite quantum state ρ_{AB} , and repeat this any number of times. Alice performs on her subsystem a measurement chosen from the set of POVMs $\{\mathcal{F}^{(m)}\}_{m=1}^M$. Hence, the actual state of Bob's subsystem is conditioned on Alice's result. Bob's conditioned state is subjected to a measurement chosen accordingly from the set $\{\mathcal{E}^{(m)}\}_{m=1}^M$. Using the generated probabilities and classical side information from Alice, Bob obtains the conditional entropies $H_1(\mathcal{E}^{(m)}|\mathcal{F}^{(m)})$ due to (2.2). The authors of [29] developed the question how to derive quantum steering inequalities on the base of entropic uncertainty relations. One of conditions implies that state-independent uncertainty relations should be used. Other conditions are clearly valid for the standard entropic functions. As was already mentioned, validity of the lower entropic bounds (3.21) and (3.22) for all states should be checked in each concrete example. If they really provide a state-independent formulation, then

we have the steering inequalities

$$\frac{1}{M} \sum_{m=1}^M H_1(\mathcal{E}^{(m)}|\mathcal{F}^{(m)}) \geq \sum_{s=1}^t a_t^{(s)} \Upsilon^{1-s} \ell^{1-s} d^s \mathcal{D}_d^{(s)} - \ln \Upsilon, \quad (3.30)$$

$$\frac{1}{M} \sum_{m=1}^M H_1(\mathcal{E}^{(m)}|\mathcal{F}^{(m)}) \geq \sum_{s=1}^n \tilde{a}_n^{(s)} \Upsilon^{1-s} \ell^{1-s} d^s \mathcal{D}_d^{(s)} - \ln \Upsilon, \quad (3.31)$$

where $\Upsilon = \min\{M \Upsilon_{K-1}^{(t)}(K^{1-t} d^t \mathcal{D}_d^{(t)}), 1\}$ and $n = \min\{t, 15\}$. The examples considered witness that the two-sided estimates (3.14) and (3.15) give better results in the case of single assigned POVM. Apparently, the same feature characterizes entropic steering inequalities (3.30) and (3.31).

IV. CONCLUDING REMARKS

We considered methods to derive two-sided estimates on the Shannon entropy by means of polynomial functions. The first way is based on truncated expansions of the Taylor type. It leads to results that are intuitively clear and easy to prove. The second way uses expansions with flexible coefficients. The significance of such expansions in applied analysis was emphasized by Lanzos [21]. As a result, we have arrived at a family of polynomials whose coefficients are connected with the shifted Chebyshev polynomials. Overall, this way provides more balanced estimates. On the other hand, the validity of obtained estimates seem to be difficult for analytical proof. Even so, the proposed two-sided estimates with limited powers can be checked numerically. Near the least points of the interval of approximation, analytical tools showed the desired correctness. It turned out that polynomials of moderate degree are often sufficient to reach enough good results. An analytical proof of the conjectured inequalities for arbitrary finite degree remains an open question. Any advances to reveal the nature of polynomial estimates with flexible coefficients will be welcome.

Initial motivation to consider polynomial estimates on the Shannon entropy comes from the question of characterizing uncertainty in special quantum measurements. Recently, quantum designs are actively studied due to nice properties useful in quantum information processing. The derived two-sided estimates were applied to formulate uncertainty and certainty relations for design-structured POVMs. A quality of new complementarity relations is characterized by comparing with the lower entropic bounds following from information diagrams. In general, new relations lead to stronger inequalities in application to the case of single assigned POVM. As well, an actual degree of the corresponding polynomial should not be very low. It is natural due to increase number of restrictions imposed on generated probabilities. So, the proposed approach allows us to take into account several given indices of the form (2.4). It was also exemplified that further improvements seem to be achievable. Maybe, information diagrams with more indices could be used for these purposes. However, such diagrams will be very complicated to examine.

Appendix A: Some properties of Chebyshev polynomials

The Chebyshev polynomials of the first kind are defined in terms of the ordinary generating function (see, e.g., item 22.9.9 in table 22.9 of [30])

$$\sum_{n=0}^{\infty} T_n(\xi) \tau^n = \frac{1 - \tau\xi}{1 - 2\tau\xi + \tau^2}. \quad (A1)$$

Other generating functions are used as well, but the formula (A1) is sufficient for our purposes. In the main text, we refer to the shifted Chebyshev polynomials of the first kind defined as

$$T_n^*(x) = T_n(2x - 1), \quad (A2)$$

where $x \in [0, 1]$. The representation as a finite sum reads as (see, e.g., §VII.8 in the book [21])

$$T_n^*(x) = \sum_{s=0}^n c_n^{(s)} x^s, \quad (A3)$$

$$c_n^{(s)} = (-1)^{n+s} 2^{2s-1} \left[2 \binom{n+s}{n-s} - \binom{n+s-1}{n-s} \right]. \quad (A4)$$

In particular, one has $c_n^{(0)} = (-1)^n$ and $c_n^{(1)} = (-1)^{n+1} 2n^2$. For convenience, exact values of $c_n^{(s)}$ for $2 \leq s \leq n$ up to $n = 15$ are presented in Table I.

TABLE I: Coefficients of the shifted Chebyshev polynomials for $2 \leq s \leq n \leq 15$.

$c_n^{(s)}$	2	3	4	5	6	7	8
	9	10	11	12	13	14	15
2	8						
3	-48	32					
4	160	-256	128				
5	-400	1120	-1280	512			
6	840	-3584	6912	-6144	2048		
7	-1568	9408	-26880	39424	-28672	8192	
8	2688	-21504	84480	-180224	212992	-131072	32768
9	-4320	44352	-228096	658944	-1118208	1105920	-589824
	131072						
10	6600	-84480	549120	-2050048	4659200	-6553600	5570560
	-2621440	524288					
11	-9680	151008	-1208064	5637632	-16400384	30638080	-36765696
	27394048	-11534336	2097152				
12	13728	-256256	2471040	-14057472	50692096	-120324096	190513152
	-199229440	132120576	-50331648	8388608			
13	-18928	416416	-4759040	32361472	-141213696	412778496	-825556992
	1133117440	-1049624576	627048448	-218103808	33554432		
14	25480	-652288	8712704	-69701632	361181184	-1270087680	3111714816
	-5369233408	6499598336	-5402263552	2936012800	-939524096	134217728	
15	-33600	990080	-15275520	141892608	-859955200	3572121600	-10478223360
	22052208640	-33426505728	36175872000	-27262976000	13589544960	-4026531840	536870912

Appendix B: On derivatives of the function (2.20)

In this sections, we derive some expressions for the first and second derivatives of $g_n(x)$. Differentiating (2.20) with respect to x and substituting $x = 1$, one has

$$g'_n(1) = \frac{(-1)^n}{2n^2} \sum_{s=2}^n c_n^{(s)} = \frac{(-1)^n}{2n^2} [T_n^*(1) - c_n^{(0)} - c_n^{(1)}] = \frac{(-1)^n - 1 + 2n^2}{2n^2}, \quad (\text{B1})$$

where we used $T_n^*(1) = T_n(1) = 1$. The same derivative taken for $x = 0$ reads as

$$g'_n(0) = \frac{(-1)^{n+1}}{2n^2} \sum_{s=2}^n \frac{c_n^{(s)}}{s-1}. \quad (\text{B2})$$

Negativity of (B2) is not obvious, since the coefficients $c_n^{(s)}$ have alternating signs. To get another representation for (B2), we write indefinite integral

$$\int \frac{T_n^*(x) - c_n^{(0)} - c_n^{(1)}x}{x^2} dx = \sum_{s=2}^n \frac{c_n^{(s)} x^{s-1}}{s-1} + \text{const}. \quad (\text{B3})$$

Multiplying the left-hand side of (B3) by τ^n and summing with respect to n , we have

$$\int \left[\frac{1 - \tau\xi}{1 - 2\tau\xi + \tau^2} - \sum_{n=0}^{\infty} (c_n^{(0)} + c_n^{(1)}x)\tau^n \right] \frac{dx}{x^2}, \quad (\text{B4})$$

where $\xi = 2x - 1$. Substituting $c_n^{(0)} = (-1)^n$ and $c_n^{(1)} = (-1)^{n+1}2n^2$, elementary calculations allow us to rewrite (B4) in the form

$$\frac{2(\tau^2 - \tau)}{(1 + \tau)^3} \ln \left| \frac{(1 + \tau)^2}{4\tau} - x \right|. \quad (\text{B5})$$

Now, the term (B5) should be expanded into power series with respect to τ . In general, this step is complicated enough. To obtain (B2), we merely write

$$\int_0^1 \frac{T_n^*(x) - c_n^{(0)} - c_n^{(1)}x}{x^2} dx = \sum_{s=2}^n \frac{c_n^{(s)}}{s-1}, \quad (\text{B6})$$

as follows from (B3). Direct calculations finally give

$$\sum_{n=0}^{\infty} \tau^n \sum_{s=2}^n \frac{c_n^{(s)}}{s-1} = (-8) \sum_{r=1}^{\infty} r^2 (-\tau)^r \sum_{\substack{m=1 \\ m \text{ odd}}}^{\infty} \frac{\tau^m}{m}. \quad (\text{B7})$$

It is clear that the power expansion (B7) starts with the term $\propto \tau^2$. To complete the job, one should find the coefficient of τ^n in (B7) and substitute it into (B2). We refrain from presenting the details here. Doing some calculations, the results are obtained (2.22) and (2.23).

Numerical calculations witness that the function $g_n(x)$ is convex for $x \in [0, 1]$. To verify this conclusion analytically, we write

$$\frac{2n^2}{(-1)^n} x g_n''(x) = \sum_{s=2}^n c_n^{(s)} s x^{s-1} = \frac{d}{dx} [T_n^*(x) - c_n^{(1)}x]. \quad (\text{B8})$$

It is not obvious that the latter is positive. Multiplying $[T_n^*(x) - c_n^{(1)}x]$ by τ^n and summing with respect to n results in

$$\sum_{n=0}^{\infty} T_n(\xi) \tau^n - \sum_{n=0}^{\infty} c_n^{(1)} x \tau^n = \frac{1 - \tau\xi}{1 - 2\tau\xi + \tau^2} + \frac{2x(\tau^2 - \tau)}{(1 + \tau)^3}, \quad (\text{B9})$$

where we used (A1) and $c_n^{(1)} = (-1)^{n+1} 2n^2$. Differentiating (B9) with respect to x , one has

$$\sum_{n=0}^{\infty} \left[\frac{dT_n(\xi)}{dx} - c_n^{(1)} \right] \tau^n = 2 \frac{d}{d\xi} \frac{1 - \tau\xi}{1 - 2\tau\xi + \tau^2} + \frac{2(\tau^2 - \tau)}{(1 + \tau)^3} = \frac{2\tau(1 - \tau^2)}{(1 - 2\tau\xi + \tau^2)^2} + \frac{2(\tau^2 - \tau)}{(1 + \tau)^3}. \quad (\text{B10})$$

The Gegenbauer polynomials $C_n^{(\alpha)}(\xi)$ of the variable $\xi \in [-1, +1]$ can be defined via the generating function (see, e.g., item 22.9.3 in table 22.9 of [30])

$$\sum_{n=0}^{\infty} C_n^{(\alpha)}(\xi) \tau^n = \frac{1}{(1 - 2\tau\xi + \tau^2)^\alpha}. \quad (\text{B11})$$

We will use such polynomials with $\alpha = 2$. It follows that $C_n^{(2)}(0) = (-1)^r(r+1)$ for $n = 2r$ and $C_n^{(2)}(1) = (n+1)(n+2)(n+3)/6$. The right-hand side of (B10) then reduces to the form

$$2\tau(1 - \tau^2) \sum_{n=0}^{\infty} C_n^{(2)}(\xi) \tau^n + \frac{2(\tau^2 - \tau)}{(1 + \tau)^3} = \sum_{n=0}^{\infty} 2 \left[C_n^{(2)}(\xi) - C_{n-2}^{(2)}(\xi) + (-1)^{n+1}(n+1)^2 \right] \tau^{n+1}, \quad (\text{B12})$$

where one assumes $C_n^{(2)}(\xi) \equiv 0$ for negative lower indices. Finally, the second derivative of interest is represented as

$$g_n''(x) = \frac{2(-1)^n}{n^2} \frac{C_{n-1}^{(2)}(\xi) - C_{n-3}^{(2)}(\xi) + (-1)^n n^2}{\xi + 1}. \quad (\text{B13})$$

where $\xi = 2x - 1$. It follows from (B13) that $g_n''(1) = 0$ for odd n and $g_n''(1) = 2$ for even n . By doing some calculations, we have arrived at a list of explicit expressions. The second derivatives for several odd values of the index reads as

follows:

$$g_3''(x) = \frac{8}{3} (1 - \xi), \quad (\text{B14})$$

$$g_5''(x) = \frac{8}{5} (1 + 4\xi^2)(1 - \xi), \quad (\text{B15})$$

$$g_7''(x) = \frac{16}{7} (1 - 2\xi^2 + 8\xi^4)(1 - \xi), \quad (\text{B16})$$

$$g_9''(x) = \frac{16}{9} (1 + 6\xi^2 - 24\xi^4 + 32\xi^6)(1 - \xi), \quad (\text{B17})$$

$$g_{11}''(x) = \frac{8}{11} (3 - 12\xi^2 + 128\xi^4 - 320\xi^6 + 256\xi^8)(1 - \xi), \quad (\text{B18})$$

$$g_{13}''(x) = \frac{8}{13} (3 + 24\xi^2 - 256\xi^4 + 1088\xi^6 - 1792\xi^8 + 1024\xi^{10})(1 - \xi), \quad (\text{B19})$$

$$g_{15}''(x) = \frac{32}{15} (1 - 6\xi^2 + 120\xi^4 - 720\xi^6 + 1920\xi^8 - 2304\xi^{10} + 1024\xi^{12})(1 - \xi). \quad (\text{B20})$$

For several even values of the index, the second derivatives are expressed as:

$$g_2''(x) = 2, \quad (\text{B21})$$

$$g_4''(x) = 2[1 + 2\xi(\xi - 1)], \quad (\text{B22})$$

$$g_6''(x) = \frac{2}{3} [3 + 16\xi^3(\xi - 1)], \quad (\text{B23})$$

$$g_8''(x) = 2[1 + (2\xi - 8\xi^3 + 16\xi^5)(\xi - 1)], \quad (\text{B24})$$

$$g_{10}''(x) = \frac{2}{3} [5 + (80\xi^3 - 256\xi^5 + 256\xi^7)(\xi - 1)], \quad (\text{B25})$$

$$g_{12}''(x) = \frac{2}{3} [3 + (6\xi - 64\xi^3 + 384\xi^5 - 768\xi^7 + 512\xi^9)(\xi - 1)], \quad (\text{B26})$$

$$g_{14}''(x) = \frac{1}{7} [14 + (448\xi^3 - 3584\xi^5 + 11776\xi^7 - 16384\xi^9 + 8192\xi^{11})(\xi - 1)]. \quad (\text{B27})$$

Due to the above expressions, we have checked $g_n''(x) \geq 0$ for all $n = 2, \dots, 15$.

-
- [1] A. Wehrl, General properties of entropy. *Rev. Mod. Phys.* **50**, 221 (1978)
 - [2] M.M. Wilde, *Quantum Information Theory* (Cambridge University Press, Cambridge, 2017)
 - [3] P. Harremoës, F. Topsøe, Inequalities between entropy and index of coincidence derived from information diagrams. *IEEE Trans. Inf. Theory* **47**, 2944 (2001)
 - [4] C.A. Fuchs, J. van de Graaf, Cryptographic distinguishability measures for quantum-mechanical states. *IEEE Trans. Inf. Theory* **45**, 1216 (1999)
 - [5] K. Korzekwa, M. Lostaglio, D. Jennings, T. Rudolph, Quantum and classical entropic uncertainty relations. *Phys. Rev. A* **89**, 042122 (2014)
 - [6] D. Deutsch, Uncertainty in quantum measurements. *Phys. Rev. Lett.* **50**, 631 (1983)
 - [7] H. Maassen, J.B.M. Uffink, Generalized entropic uncertainty relations. *Phys. Rev. Lett.* **60**, 1103 (1988)
 - [8] S. Wehner, A. Winter, Entropic uncertainty relations – a survey. *New J. Phys.* **12**, 025009 (2010)
 - [9] P.J. Coles, M. Berta, M. Tomamichel, S. Wehner, Entropic uncertainty relations and their applications. *Rev. Mod. Phys.* **89**, 015002 (2017)
 - [10] I. Białynicki-Birula, L. Rudnicki, Entropic uncertainty relations in quantum physics. *Statistical Complexity*, pp. 1–34 (Springer, Berlin, 2011)
 - [11] A. Hertz, N.J. Cerf, Continuous-variable entropic uncertainty relations. *J. Phys. A: Math. Theor.* **52**, 173001 (2019)
 - [12] T. Durt, B.-G. Englert, I. Bengtsson, K. Życzkowski, On mutually unbiased bases. *Int. J. Quantum Inf.* **8**, 535 (2010)
 - [13] J. Renes, R. Blume-Kohout, A. Scott, C. Caves, Symmetric informationally complete quantum measurements. *J. Math. Phys.* **45**, 2171 (2004)
 - [14] A.J. Scott, Tight informationally complete quantum measurements. *J. Phys. A: Math. Gen.* **39**, 13507 (2006)
 - [15] A. Ambainis, J. Emerson, Quantum t -designs: t -wise independence in the quantum world. E-print arXiv:quant-ph/0701126 (2007)
 - [16] A. Ketterer, O. Gühne, Entropic uncertainty relations from quantum designs. *Phys. Rev. Research* **2**, 023130 (2020)
 - [17] A.E. Rastegin, Rényi formulation of uncertainty relations for POVMs assigned to a quantum design. *J. Phys. A: Math. Theor.* **53**, 405301 (2020)

- [18] T.M. Cover, J.A. Thomas, Elements of Information Theory (John Wiley & Sons, New York, 2006)
- [19] C. Tsallis, Possible generalization of Boltzmann–Gibbs statistics. *J. Stat. Phys.* **52**, 479 (1988)
- [20] I. Bengtsson, K. Życzkowski, Geometry of Quantum States: An Introduction to Quantum Entanglement (Cambridge University Press, Cambridge, 2017)
- [21] C. Lanczos, Applied Analysis (Dover, New York, 2010)
- [22] A.E. Rastegin, Uncertainty relations for MUBs and SIC-POVMs in terms of generalized entropies. *Eur. Phys. J. D* **67**, 269 (2013)
- [23] B. Vermersch, A. Elben, M. Dalmonte, J.I. Cirac, P. Zoller, Unitary n -designs via random quenches in atomic Hubbard and spin models: Application to the measurement of Rényi entropies. *Phys. Rev. A* **97**, 023604 (2018)
- [24] S. Wu, S. Yu, K. Mølmer, Entropic uncertainty relation for mutually unbiased bases. *Phys. Rev. A* **79**, 022104 (2009)
- [25] R.H. Hardin, N.J.A. Sloane, McLaren’s improved snub cube and other new spherical designs in three dimensions. *Discrete Comput. Geom.* **15**, 429 (1996)
- [26] A.D. McLaren, Optimal numerical integration on a sphere. *Math. Comp.* **17**, 361 (1963)
- [27] H.M. Wiseman, S.J. Jones, A.C. Doherty, Steering, entanglement, nonlocality, and the Einstein-Podolsky-Rosen paradox. *Phys. Rev. Lett.* **98**, 140402 (2007)
- [28] R. Uola, A.C.S. Costa, H.C. Nguyen, O. Gühne, Quantum steering. *Rev. Mod. Phys.* **92**, 15001 (2020)
- [29] T. Kriváchy, F. Fröwis, N. Brunner, Tight steering inequalities from generalized entropic uncertainty relations. *Phys. Rev. A* **98**, 062111 (2018)
- [30] M. Abramowitz, I.A. Stegun, eds., Handbook of Mathematical Functions: with Formulas, Graphs, and Mathematical Tables (Dover, New York, 1972)